MADRID 2015
1-4 June 2015 | IFEMA Madrid

We P3 09

Robust Simultaneous Time-lapse Full-waveform Inversion with Total-variation Regularization of Model Difference

M. Maharramov* (Stanford University) & B. Biondi (Stanford University)

SUMMARY

We present a technique for reconstructing production-induced subsurface velocity model changes from time-lapse seismic data using full-waveform inversion (FWI). The technique is based on simultaneously inverting multiple survey vintages with model-difference regularization using the total-variation (TV) seminorm. We compare the new TV-regularized time-lapse FWI with the joint time-lapse FWI from our earlier work and the popular sequential difference method. We tested the proposed method on synthetic datasets that exhibit survey repeatability issues. The results demonstrate advantages of the proposed TV-regularized simultaneous inversion over alternative methods for recovering production-induced velocity changes, achieved by preserving sharp contrasts and reducing oscillatory artifacts.

Introduction

Conventional time-lapse seismic processing techniques rely on picking time displacements and changes in reflectivity amplitudes between migrated baseline and monitor images, and converting them into impedance changes and subsurface deformation. This approach requires a significant amount of expert interpretation and quality control. Wave-equation image-difference tomography is a more automatic alternative method to recover velocity changes (Albertin et al., 2006) that allows localized target-oriented inversion of model perturbations (Maharramov and Albertin, 2007). Another alternative is based on using the high-resolution power of the full-waveform inversion (Sirgue et al., 2010) to reconstruct production-induced changes from wide-offset seismic acquisitions (Routh et al., 2012; Zheng et al., 2011; Asnaashari et al., 2012; Raknes et al., 2013; Maharramov and Biondi, 2014b; Yang et al., 2014). However, time-lapse FWI is sensitive to repeatability issues (Asnaashari et al., 2012), with both coherent and incoherent noise potentially masking important production-induced changes. The joint time-lapse FWI proposed in (Maharramov and Biondi, 2014b) addresses repeatability issues by joint inversion of multiple vintage with model-difference regularization based on the L_2-norm and produced improved results when compared to the conventional time-lapse FWI techniques. In this work we extend this joint inversion approach to include edge-preserving total-variation (TV) model-difference regularization (Maharramov and Biondi, 2014c). We show that the new method can achieve a dramatic improvement over alternative techniques by significantly reducing oscillatory artifacts in the recovered model difference, and we demonstrate this on a synthetic dataset with added noise.

Method

FWI applications in time-lapse problems seek to recover induced changes in the subsurface model using multiple seismic datasets from different acquisition vintages. For two surveys sufficiently separated in time, we call such datasets (and the associated models) "baseline" and "monitor". Time-lapse FWI can be carried out by separately inverting the baseline and monitor models ("parallel difference") or inverting them sequentially with, e.g., the baseline supplied as a starting model for the monitor inversion ("sequential difference"). The latter may achieve a better recovery of model differences in the presence of incoherent noise (Asnaashari et al., 2012; Maharramov and Biondi, 2014b). Another alternative is to apply the "double-difference" method (Watanabe et al., 2004; Denli and Huang, 2009; Zheng et al., 2011; Asnaashari et al., 2012; Raknes et al., 2013). The latter approach may require significant data preprocessing and equalization (Asnaashari et al., 2012; Maharramov and Biondi, 2014b) across survey vintages.

In all of these techniques, optimization is carried out with respect to one model at a time, albeit of different vintages at different stages of the inversion. We propose to invert the baseline and monitor models simultaneously by solving the following optimization problem:

$$\alpha\|\mathbf{u}_b(\mathbf{m}_b)-\mathbf{d}_b\|_2^2+\beta\|\mathbf{u}_m(\mathbf{m}_m)-\mathbf{d}_m\|_2^2+ \quad (1)$$

$$\delta\|\mathbf{WR}(\mathbf{m}_m-\mathbf{m}_b)\|_1 \;\rightarrow\; \min \quad (2)$$

with respect to both the baseline and monitor models $\mathbf{m}_b$ and $\mathbf{m}_m$. Problem (1,2) describes time-lapse FWI with the L_1 regularization of a transformed model difference (2). The terms (1) correspond to separate baseline and monitor inversions with observed data $\mathbf{d}$ and modeled data $\mathbf{u}$. This approach differs from our earlier approach proposed in (Maharramov and Biondi, 2014b) by using L_1-norm regularization in (2) instead of L_2-norm based regularization. In (2), $\mathbf{R}$ and $\mathbf{W}$ denote regularization and weighting operators respectively. If $\mathbf{R}$ is the gradient magnitude operator

$$\mathbf{R}f(x,y,z) \;=\; \sqrt{f_x^2+f_y^2+f_z^2}, \quad (3)$$

then (2) becomes the "Total Variation" (TV) seminorm (Ziemer, 1989). The latter case is of particular interest as minimization of the gradient L_1 norm promotes "blockiness" of the model-difference, potentially reducing oscillatory artifacts (Rudin et al., 1992; Aster et al., 2012).

The model difference regularization weights **W** may be obtained from prior geomechanical information. For example, a rough estimate of production-induced velocity changes can be obtained from time shifts (Hatchell and Bourne, 2005; Barkved and Kristiansen, 2005) and used to map subsurface regions of expected production-induced perturbation. However, successfully solving the L_1-regularized problem (1,2) is less sensitive to choice of the weighting operator **W**. For example, we show below that the TV-regularization using (3) with $\mathbf{W} = 1$ recovers non-oscillatory components of the model difference, while the L_2 approach would result in either smoothing or uniform reduction of the model difference.

In addition to the fully simultaneous inversion, Maharramov and Biondi (2013, 2014b) proposed and tested a "cross-updating" technique that offers a simple but remarkably effective approximation to minimizing the objective function (1), while obviating the difference regularization and weighting operators **R** and **W**. This technique consists of one standard run of the sequential difference algorithm, followed by a second run with the inverted monitor model supplied as the starting model for the second baseline inversion

$$\begin{aligned}\mathbf{m}_{\text{INIT}} \rightarrow &\text{baseline inversion} \rightarrow \text{monitor inversion} \rightarrow \\ &\text{baseline inversion} \rightarrow \text{monitor inversion},\end{aligned} \tag{4}$$

and computing the difference of the latest inverted monitor and baseline models. Cross-updating and the simultaneous inversion with L_2-based model difference regularization yielded qualitatively similar results within the inversion target (Maharramov and Biondi, 2014b). In this paper we compare the results of applying the sequential difference and cross-updating against simultaneous inversion with a TV-regularized model difference (1,2,3), and demonstrate the ability of the new approach to preserve sharp contrasts and reduce oscillatory artifacts.

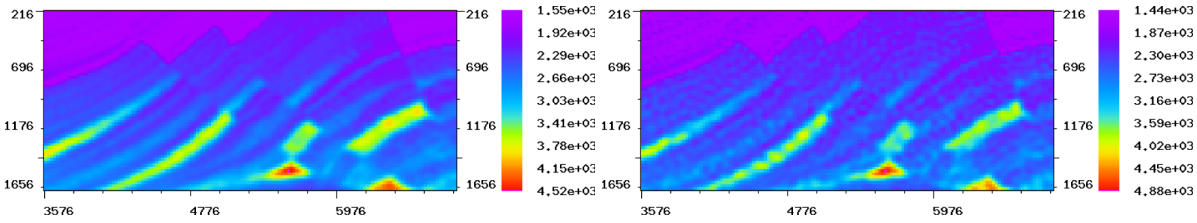

Figure 1 *Left) Target area of the baseline model inverted from a clean synthetic. Right) Target area of the baseline model inverted from a 7 dB SNR synthetic. In both cases the baseline model is reconstructed reasonably well, however, errors due to noise are comparable in magnitude to production-induced effects.*

Example

The Marmousi velocity model is used as a baseline, over a 384×122 grid with a 24 m grid spacing. Production-induced velocity changes are modeled as a negative -200 m/s perturbation at about 4.5 km inline 800 m depth, and a positive 300 m/s perturbation at 6.5 km inline, 1 km depth, illustrated in Figure 2. While the whole Marmousi model is inverted, only model differences for the section between the approximate inline coordinates 3.5 km and 7 km to the depth of approximately 1.7 km are shown here. The inversion is carried out in the frequency domain for 3.0, 3.6, 4.3, 5.1, 6.2, 7.5, 9.0, 10.8, 12.8, and 15.5 Hz, where the frequencies are chosen based on the estimated offset to depth range of the data (Sirgue and Pratt, 2004). The baseline acquisition has 192 shots at a depth of 16 m with a 48 m spacing, and 381 receivers at a depth of 15 m with a 24 m spacing. The minimum offset is 48 m. The source function is a Ricker wavelet centered at 10.1 Hz. Absorbing boundary conditions are applied along the entire model boundary, including the surface (thus suppressing multiples). A smoothed true model is used as a starting model for the initial baseline inversion. The smoothing is performed using a triangular filter with a 20-sample half-window in both vertical and horizontal directions. Random Gaussian noise is added to the noise-free synthetic data to produce a noisy dataset with 7 dB signal-to-noise ratio. The results of baseline model inversion from the clean and 7 dB SNR synthetic data are

shown in Figure 1. The noisy monitor dataset is generated for the model perturbation of Figure 2 Left), using the same acquisition geometry and source wavelet. Results for model difference inversion from the 7 dB SNR synthetic datasets using various methods are shown in Figures 2 and 3. The model-difference regularization weights **W** in (2) are set to 1 everywhere in the modeling domain. The two terms in (1) are of the same magnitude and therefore α and β are set to 1. Parameter δ is set to 10^{-6} but can be varied for different acquisition source and geometry parameters. The result of the initial baseline inversion is supplied as a starting model for both $\mathbf{m}_b$ and $\mathbf{m}_m$ in the simultaneous inversion.

In all the inversions, up to 10 iterations of the nonlinear conjugate gradients algorithm (Nocedal and Wright, 2006) are performed for each frequency. However, because the L_1 component (2) of the objective function is not smooth, differentiation of (3) may result in an overflow where the gradient magnitude is very small. To avoid this, we use gradient smoothing similar to "Iteratively Re-weighted Least Squares" (Aster et al., 2012): whenever the gradient magnitude (3) is below some threshold value ε, division by (3) is substituted with division by ε. The threshold $\varepsilon = 10^{-5}$ was chosen in our experiments to be less than $|\Delta v/v^2|$, with v as the baseline model velocity within the target area, and Δv as a lower bound on production-induced velocity changes. Note that alternative solution techniques such as "Bregman iterations" (Goldstein and Osher, 2009) for TV-regularized problems can be employed in TV-regularized (time-lapse) FWI (Maharramov and Biondi, 2014a) where fixed and small ε-thresholding may adversely impact convergence.

Results

The results of applying iterated sequential difference (Maharramov and Biondi, 2014b) to the two datasets are shown in Figure 2. The corresponding cross-updating and TV-regularized simultaneous inversion results are shown in Figure 3. While cross-updating demonstrates certain robustness with regard to uncorrelated noise in the data and computational artifacts (note the quantitative improvement of the recovered difference magnitudes in the left panel of Figure 3 compared with the right panel of Figure 2), the TV-regularized simultaneous inversion (right panel of Figure 3) achieves a significant further improvement by reducing oscillatory artifacts and honoring the blocky nature of the model difference.

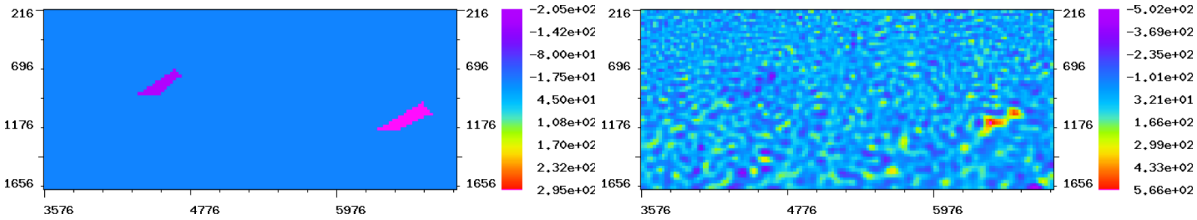

Figure 2 *Left) True velocity differences consist of a negative (−200 m/s) perturbation at about 4.5 km inline 800 m depth and a positive (300 m/s) perturbation at 6.5 km inline, 1 km depth. Right) Model difference inverted using iterated sequential difference.*

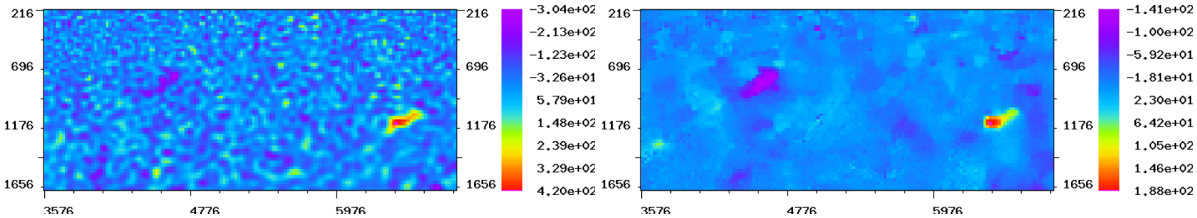

Figure 3 *Model difference recovered using Left) cross-updating, Right) simultaneous inversion with a TV-regularized model difference. Note the higher accuracy and stability to random noise of the TV-regularized simultaneous inversion.*

Conclusions

Our new TV-regularized simultaneous inversion technique is a more robust further development of previous joint inversion methods. Use of the TV regularization in the simultaneous inversion allows robust recovery of production-induced changes, and penalizes unwanted model oscillations that may mask useful production-induced changes.

Acknowledgements

The authors would like to thank Stewart Levin for a number of useful discussions, and the Stanford Center for Computational Earth and Environmental Sciences for providing computing resources.

References

Albertin, U., Sava, P., Etgen, J. and Maharramov, M. [2006] Adjoint wave-equation velocity analysis. *76th Annual International Meeting, SEG, Expanded Abstracts*, 3345–3349.

Asnaashari, A., Brossier, R., Garambois, S., Audebert, F., Thore, P. and Virieux, J. [2012] Time-lapse imaging using regularized FWI: A robustness study. *82nd Annual International Meeting, SEG, Expanded Abstracts, doi:10.1190/segam2012-0699.1*, 1–5.

Aster, R., Borders, B. and Thurber, C. [2012] *Parameter estimation and inverse problems*. Elsevier.

Barkved, O. and Kristiansen, T. [2005] Seismic time-lapse effects and stress changes: Examples from a compacting reservoir. *The Leading Edge*, **24**(12), 1244–1248.

Denli, H. and Huang, L. [2009] Double-difference elastic waveform tomography in the time domain. *79th Annual International Meeting, SEG, Expanded Abstracts*, 2302–2306.

Goldstein, T. and Osher, S. [2009] The split Bregman method for L1-regularized problems. *SIAM Journal on Imaging Sciences*, **2**(2), 323–343.

Hatchell, P. and Bourne, S. [2005] Measuring reservoir compaction using time-lapse timeshifts. *75th Annual International Meeting, SEG, Expanded Abstracts*, 2500–2503.

Maharramov, M. and Albertin, U. [2007] Localized image-difference wave equation tomography. *77th Annual International Meeting, SEG, Expanded Abstracts*, 3009–3013.

Maharramov, M. and Biondi, B. [2013] Simultaneous time-lapse full waveform inversion. *Stanford Exploration Project Report*, **150**, 63–70.

Maharramov, M. and Biondi, B. [2014a] Improved depth imaging by constrained full-waveform inversion. *Stanford Exploration Project Report*, **155**, 19–24.

Maharramov, M. and Biondi, B. [2014b] Joint full-waveform inversion of time-lapse seismic data sets. *84th Annual Meeting, SEG, Expanded Abstracts*, 954–959.

Maharramov, M. and Biondi, B. [2014c] Robust joint full-waveform inversion of time-lapse seismic datasets with total-variation regularization. *Stanford Exploration Project Report*, **155**, 199–208.

Nocedal, J. and Wright, S.J. [2006] *Numerical Optimization*. Springer.

Raknes, E., Weibull, W. and Arntsen, B. [2013] Time-lapse full waveform inversion: Synthetic and real data examples. *83rd Annual International Meeting, SEG, Expanded Abstracts*, 944–948.

Routh, P., Palacharla, G., Chikichev, I. and Lazaratos, S. [2012] Full wavefield inversion of time-lapse data for improved imaging and reservoir characterization. *82nd Annual International Meeting, SEG, Expanded Abstracts, doi:10.1190/segam2012-1043.1*, 1–6.

Rudin, L.I., Osher, S. and Fatemi, E. [1992] Nonlinear total variation based noise removal algorithms. *Physica D: Nonlinear Phenomena*, **60**(1-4), 259–268.

Sirgue, L., Barkved, O., Dellinger, J., Etgen, J., Albertin, U. and Kommendal, J. [2010] Full waveform inversion: The next leap forward in imaging at Valhall. *First Break*, **28**(4), 65–70.

Sirgue, L. and Pratt, R. [2004] Efficient waveform inversion and imaging: A strategy for selecting temporal frequencies. *Geophysics*, **69**(1), 231–248.

Watanabe, T., Shimizu, S., Asakawa, E. and Matsuoka, T. [2004] Differential waveform tomography for time-lapse crosswell seismic data with application to gas hydrate production monitoring. *74th Annual International Meeting, SEG, Expanded Abstracts*, 2323–2326.

Yang, D., Malcolm, A.E. and Fehler, M.C. [2014] Time-lapse full waveform inversion and uncertainty analysis with different survey geometries.

Zheng, Y., Barton, P. and Singh, S. [2011] Strategies for elastic full waveform inversion of time-lapse ocean bottom cable (OBC) seismic data. *81st Annual International Meeting, SEG, Expanded Abstracts*, 4195–4200.

Ziemer, W.P. [1989] *Weakly Differentiable Functions: Sobolev Spaces and Functions of Bounded Variation*. Springer.